

A Superior High-Strength Dilute Mg-Bi-Ca Extrusion Alloy with a Bimodal Microstructure

Shuaiju Meng^{1,2,3,*}, Mingchi Zhang^{1,3}, Haoran Xiao^{1,4}, Zhanju Luo³, Wei Yu^{5,*}, Runlin Jiang³, Xueqi Cheng³ and Lidong Wang^{1,3,*}

¹ State Key Laboratory of Advanced Processing and Recycling of Nonferrous Metals, Lanzhou University of Technology, Lanzhou 730050, China; zmclut2457706839@163.com (M.Z.); X19506599932@163.com (H.X.)

² Engineering Research and Development Institute, CITIC Dicastal Co., Ltd., Qinguangdao 066011, China

³ School of Materials Science and Engineering, Lanzhou University of Technology, Lanzhou 730050, China; lzjaqq2022@163.com (Z.L.); jrl18770873294@163.com (R.J.); X3160471139@163.com (X.C.)

⁴ College of Electromechanical Engineering, Qingdao University of Science and Technology, Qingdao 266061, China

⁵ School of Materials Science and Engineering, Hefei University of Technology, Hefei 200039, China

* Correspondence: shuaijumeng@163.com (S.M.); yuwei52213@163.com (W.Y.); wangld@lut.edu.cn (L.W.)

Abstract: Improving the mechanical properties of Mg alloys is of great significance for their wide application. A micro-alloyed Mg-1.45Bi-0.79Ca alloy (in wt.%) exhibiting a high tensile yield strength of 394 ± 5 MPa and a moderate elongation of $6.6 \pm 0.6\%$ was fabricated by single pass extrusion. The superior high strength is mainly attributed to the synergy effects of ultra-fine dynamic recrystallized grains; numerous Mg₂Ca, Mg₃Bi₂, and Mg₂Bi₂Ca nano-precipitates; residual dislocations; sub-grain boundaries; as well as strong <10-10> fibre texture in the extrusion direction.

Keywords: Mg alloy; extrusion; microstructure; dynamic recrystallization; mechanical properties



Citation: Meng, S.; Zhang, M.; Xiao, H.; Luo, Z.; Yu, W.; Jiang, R.; Cheng, X.; Wang, L. A Superior High-Strength Dilute Mg-Bi-Ca Extrusion Alloy with a Bimodal Microstructure. *Metals* **2022**, *12*, 1162. <https://doi.org/10.3390/met12071162>

Academic Editors: Jianyue Zhang and Alan Luo

Received: 12 June 2022

Accepted: 5 July 2022

Published: 7 July 2022

Publisher's Note: MDPI stays neutral with regard to jurisdictional claims in published maps and institutional affiliations.



Copyright: © 2022 by the authors. Licensee MDPI, Basel, Switzerland. This article is an open access article distributed under the terms and conditions of the Creative Commons Attribution (CC BY) license (<https://creativecommons.org/licenses/by/4.0/>).

1. Introduction

Thanks to their low density, good castability, high damping capacity, and good biocompatibility, Mg alloys have shown significant application potential in transportation, biomedical industries, and other fields [1,2]. However, the strength of commercial high-strength Mg alloys such as AZ80 and ZK60 is still much lower than that of wrought Al alloys such as 2024 and 7075 [3]. Besides, the low corrosion resistance [4] and significant plastic anisotropy [5] also retard the wide application of wrought magnesium alloys. In terms of strength, it is clear that further improvement of the mechanical properties of Mg alloys is of great significance on their way to becoming a commercial alternative to Al alloys and steel.

It is reported that alloying Mg with rare-earth elements (REs) such as Gd and Y is an effective method for achieving high strength and moderate ductility [6]. However, the increase in cost caused by RE addition is a major obstacle to their commercial application. In order to promote application, some new low-cost, high-strength RE-free Mg alloys, such as Mg-Al- [7,8] and Mg-Sn-based [2,9] alloys, have been fabricated. Pan et al. developed an Mg-2Sn-2Ca (TX22, all compositions quoted in this work are in wt.%) alloy [9] with very fine grains exhibiting an ultra-high tensile yield strength (TYS) of 443 MPa. Similar to the Mg-Sn-based alloy, the Mg-Bi-based alloy, as a typical precipitation-type phase equilibrium, also demonstrates great potential in developing RE-free high-strength extrudable materials [2]. Besides, Bi element is non-toxic and is called “green metal” [10], and its price is much lower than that of RE and Sn. Recently, several Mg-Bi-based alloys with attractive mechanical properties have been fabricated. It is reported that, when 3–8% Bi is added to pure Mg, the TYS of the extruded samples can be increased by 88 MPa to 129 MPa, mainly because of the grain refinement and precipitation strengthening by fine Mg₃Bi₂

phases [11,12]. Additionally, Al, Zn, Sn, Ca, and Mn have been introduced into Mg-Bi-based alloys to improve their mechanical properties [13–20]. For example, by alloying an Mg-Bi-based alloy with Al and Zn, an extruded Mg-8Bi-1Al-1Zn (BAZ811) alloy exhibiting a TYS of 291 MPa and an elongation of 14.6% was fabricated in our former research [13]. More recently, alloying Mg-Bi alloys with Sn was also used to further increase their mechanical properties. An as-extruded Mg-5Bi-6Sn alloy having typical basic fiber texture and partial dynamic recrystallization (DRX) microstructure exhibits a TYS of 264 MPa [14]. Furthermore, researchers have found that the addition of Ca will also significantly affect the microstructure and properties of the Mg-Bi-based alloys. W.L. Cheng et al. [15] found that the average grain size and intensity of the texture of the extruded Mg-1Bi-1Al alloy can be significantly affected by the addition of different contents of Ca. S. Remennik et al. [16] developed a new type of ductile Mg-Bi-Ca alloy with an ultimate tensile strength of 205 MPa and elongation (EL) of 40% by combining rapid solidification and hot extrusion. Inspired by this study, our former studies [17,18] further found that high ductile Mg-Bi-Ca alloys with elongation over 43% can be fabricated by the one-pass extrusion process. However, the TYS of all the Mg-Bi-based alloys that have been fabricated up to now is still less than 360 MPa, thus the strength of Mg-Bi-based alloys urgently needs to be improved.

In this study, a new low-cost micro-alloyed Mg-Bi-Ca alloy with an ultra-high TYS was successfully fabricated by single pass extrusion, and the related microstructure and mechanical properties were systematically investigated and discussed.

2. Materials and Methods

The alloy ingot with an analysis composition of Mg-1.45Bi-0.79Ca (denoted as BX11) was fabricated by melting high purity Mg, Bi, and Mg-20Ca master alloy and gravity casting. The as-cast BX11 alloy with a dimension of $\text{Ø}60 \text{ mm} \times 150 \text{ mm}$ was homogenized at 480 °C for 5 h, and then extrusion processing was carried out at 280 °C with an extrusion ratio of 36:1 at an exit speed (V_{exit}) of 4 mm/s. Microstructure and texture characterizations were conducted using an Olympus BX51M optical microscope (OM, OLYMPUS, Tianjin, China), scanning electron microscopy (SEM, JEOL JSM-7000F, JEOL, Tianjin, China), energy dispersive spectrometer (EDS), electron back-scatter diffraction (EBSD), and transmission electron microscope (TEM) equipped with energy-dispersive X-ray spectroscopy (EDX). The dog-bone-shaped specimens with the gauge dimension of $\text{Ø}5.5 \text{ mm} \times 32 \text{ mm}$ were introduced for room temperature tensile tests, which were performed along the extrusion direction (ED) using the SUNS-UTM5105X mechanical testing machine (SHENZHEN SUNS TECHNOLOGY STOCK CO., LTD., Tianjin, China) with an initial strain rate of $1 \times 10^{-3} \text{ s}^{-1}$. The dimensions of samples used in room temperature tensile test and the specimen after/before fracture are presented in Figure 1a,b, respectively. Three samples of BX11 alloy were tested to ensure the consistency of the mechanical properties and the average values and corresponding standard deviations were obtained for the sake of simplicity.

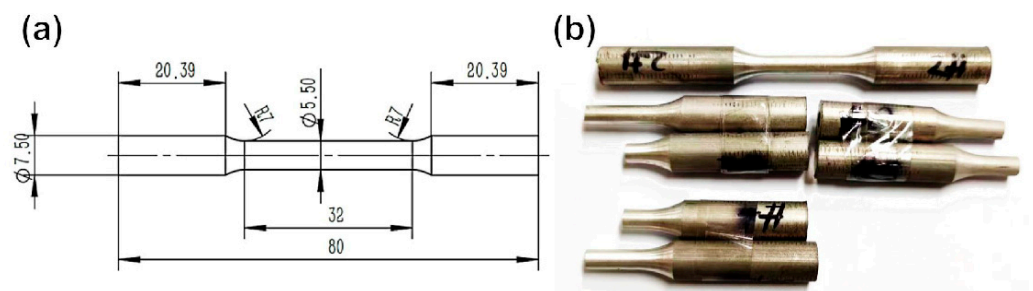


Figure 1. Dimensions of samples used in room temperature tensile test (a) and the specimen after/before fracture (b).

3. Results and Discussion

Figure 2 indicates OM and SEM images of the as-extruded BX11 alloy. Generally, the alloy exhibits a bimodal microstructure consisting of fine dynamic recrystallized (DRXed) grains and elongated unDRXed grains, as circled in red in Figure 2b. The volume fraction of the unDRXed grains is ~45%. As shown in Figure 2a,c, a small amount of micro-scale white second particles can be detected distributed along the ED in the matrix, which were further characterized as Mg-Bi, Mg-Bi-Ca, and Mg-Ca intermetallics by the EDS results in Figure 2d. The particles containing the same elements were identified as Mg_3Bi_2 , Mg_2Bi_2Ca , and Mg_2Ca phases, respectively, in previously reported Mg-Bi-Ca alloys [17–19].

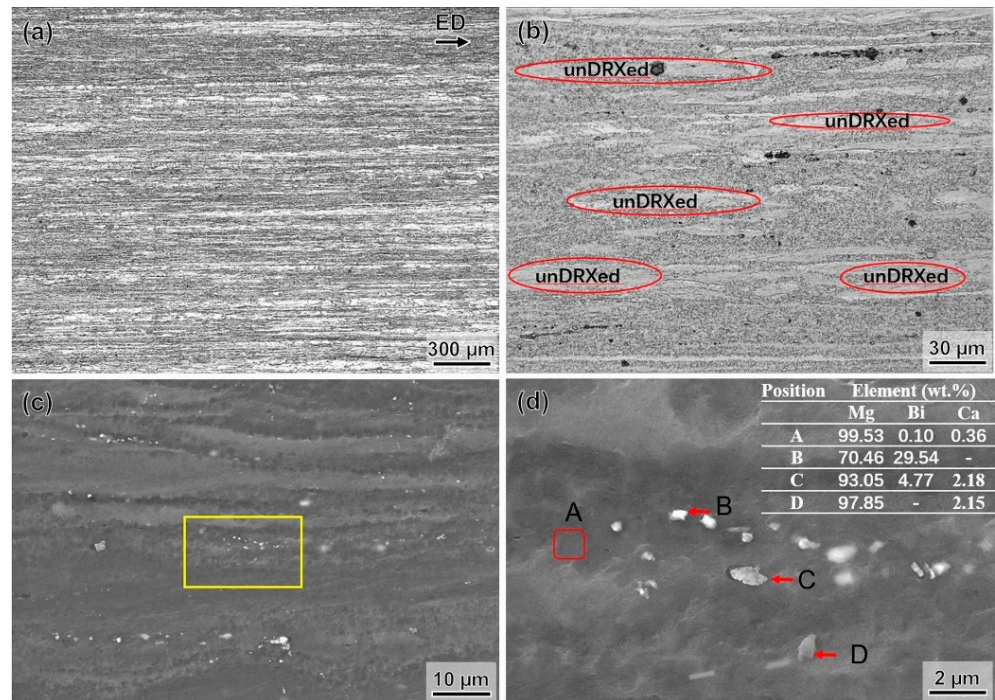


Figure 2. OM (a,b) and SEM (c,d) micrographs of the as-extruded BX11 alloy.

Figure 3 shows the EBSD analysis results of the as-extruded BX11 sample. Both the coarse elongated grains with an average grain size (AGS.) of ~9.8 μm and fine grains with a diameter of ~0.95 μm can be seen clearly in the inverse pole figure (IPF) maps, forming a bimodal microstructure, which is well agreed upon with OM and SEM observation. In addition, the BX11 alloy exhibits a basal fiber texture (see Figure 3d–f), which means that the {0001} plane and the $\langle 10\bar{1}0 \rangle$ direction are mainly oriented parallel to the ED. It should be noted that the unDRXed grains demonstrate strong texture with $\langle 10\bar{1}0 \rangle // \text{ED}$, while a more randomized texture is generated and two preferred orientations of both $\langle 10\bar{1}0 \rangle // \text{ED}$ and $\langle 2\bar{1}10 \rangle // \text{ED}$ can be detected with the fine DRXed grains. The result is consistent with previous works of the texture components' transition during DRX [11,13]. Interestingly, necklace-like structure with fine DRXed grains formed around the elongated grains can be readily observed in the microstructure, indicating that the discontinuous DRX (DDRX) happened during extrusion. It should be emphasized that the basal texture intensity of the BX11 alloy is much higher than that of the high-alloyed Mg-8Bi-1Al-1Zn [13], low-temperature and slow-speed ($T = 200\text{ }^\circ\text{C}$, $V_{\text{exit}} = 0.084\text{ m/min}$) extruded AZ80 [21], and high-speed ($T = 300\text{ }^\circ\text{C}$, $V_{\text{exit}} = 13\text{ m/min}$) extruded Mg-Bi-Ca alloy [17], indicating that the texture of the extruded Mg samples greatly depends on both the alloy composition and its processing parameters, including temperature and speed. The mechanism of texture evolution in Mg-Bi-Ca alloys prepared under different extrusion parameters needs to be further systematically studied.

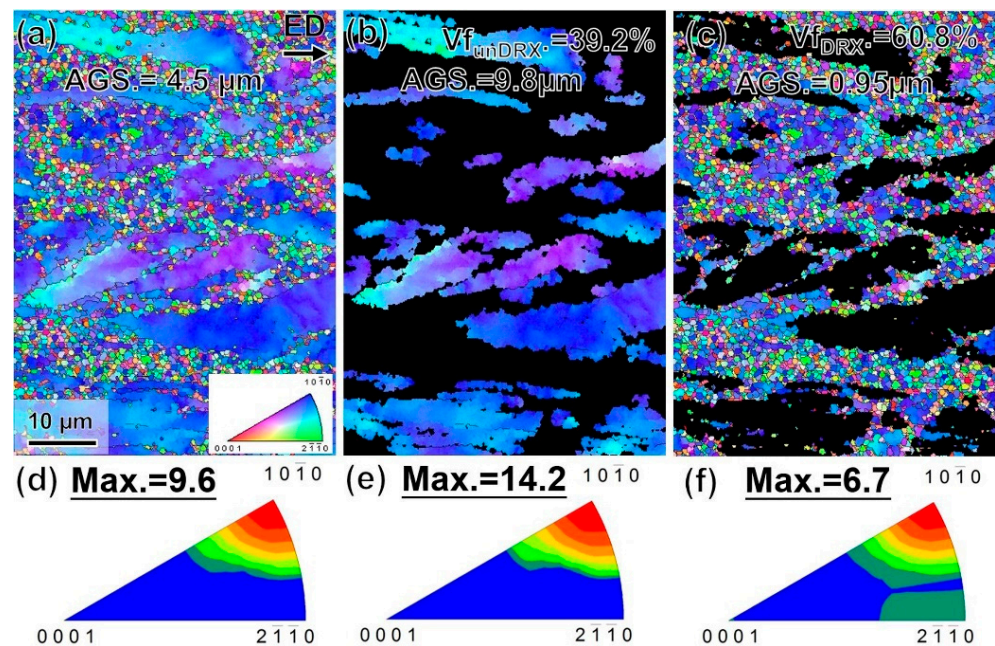


Figure 3. Inverse pole figure maps (a–c) and corresponding inverse pole figure (d–f) of as-extruded BX11 alloy: (a,d) overall, (b,e) unDRXed, and (c,f) DRXed regions.

In order to further reveal its precipitation behavior, TEM images and EDX results of the as-extruded BX11 alloy are presented in Figure 4. Numerous nano-precipitates can be found distributed homogeneously in the matrix, as circled by the red ellipses in Figure 4b, and most of the precipitates are enrich with Mg and Ca, which is consistent with the result observed in the high-speed extruded Mg-1.32Bi-0.72Ca alloy, and these precipitates were confirmed to be Mg_2Ca phases [17]. Besides, some precipitates are found to stay nearby the residual dislocation lines, indicating that the dislocations may provide preferred nucleation sites for the nano-precipitates. Moreover, high densities of the residual dislocations are readily detected and these dislocations have partially transformed into sub-grains and occupied the original grain interiors in the manner of continuous DRX (CDRX), as indicated by the yellow arrows in Figure 4a,b. These sub-grains nearby the unDRXed region have a size of ~ 100 nm, suggesting that the residual dislocations introduced by slow speed extrusion play a critical role in generating the potential nuclei of recrystallization. Figure 4c,d show more typical DRXed grains and most of them exhibit a grain size of ~ 0.55 μm . Apart from Mg_2Ca particles, the ternary Mg-Bi-Ca phase and binary Mg-Bi phase are also detected in the BX11 alloy, as shown in Figure 4c,d. The particles containing the same elements were identified as Mg_2Bi_2Ca and Mg_3Bi_2 in other Mg-5Bi-1Ca alloys [16] and the high-speed extruded Mg-1.32Bi-0.72Ca alloy [17], respectively.

According to the SEM and TEM images, it can be found that there are numerous nano-scale Mg_2Ca , Mg_3Bi_2 , and Mg_2Bi_2Ca precipitates and a small amount of micro-scale Mg_2Bi_2Ca and Mg_2Ca particles in the as-extruded BX11 alloy. During hot extrusion, all of these nano-scale precipitates and fine micro-scale particles (~ 1 μm) can substantially retard DRX by greatly reducing the mobility of grain boundaries and inhibiting boundary bulging required for the nucleation of new DRXed grains, which is known as the Zener pinning effect [12,13]. On the one hand, this suppression of DRX eventually leads to partial dynamic recrystallization of the BX11 alloy, forming a bimodal structure. On the other hand, these fine particles can also inhibit the growth of DRXed grains through the grain-boundary pinning effect, thereby resulting in considerable grain refinement of the DRXed grains in BX11. As a result, the ultra-fine DRXed grains (~ 0.55 μm) in the BX11 alloy, which is formed through both DDRX along grain boundaries and CDRX in the grain interior and effectively pinned by fine particles, is comparable to that in ultra-high strength TX22 [9], and much smaller than that of the BAZ811 [13] and Mg-Bi-Mn alloy [20]. Accordingly, high strength

can be expected in the BX11 alloy based on the ultra-fine DRXed grains, nano-particles including Mg_2Ca , Mg_2Bi_2Ca and Mg_3Bi_2 , residual dislocations, and sub-grain boundaries in its microstructure.

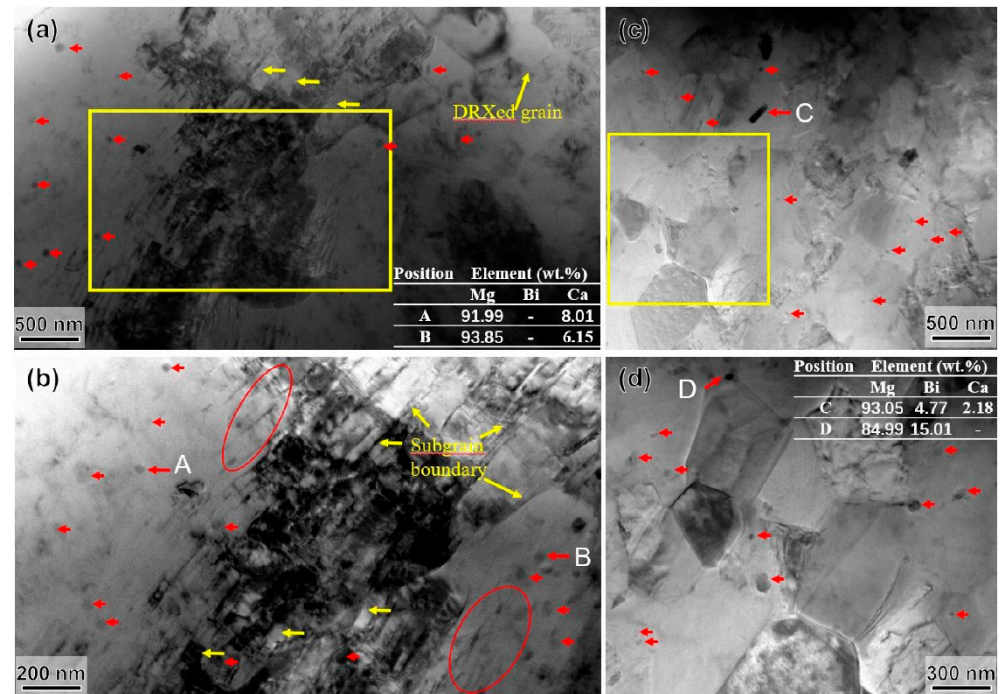


Figure 4. TEM bright field images of the (a,b) elongated region and (c,d) DRXed region of the as-extruded BX11 alloy.

The tensile properties including TYS, ultimate tensile strength (UTS), and EL of the as-extruded BX11 alloy are summarized in Table 1, compared with AZ31 [13] and some other typical RE-free Mg alloys [9,11,12]. The typical tensile stress–strain curves of the as-extruded BX11 alloy are represented in Figure 5, compared with pure Mg and AZ31 extruded under similar conditions [13]. The as-extruded BX11 alloy shows a TYS of 394 ± 5 MPa and acceptable elongation of $\sim 6.6 \pm 0.6\%$. As compared in Table 1, the TYS of the BX11 sample is much higher than that of commercial AZ31 alloy [13] and high-speed extruded Mg-1.32Bi-0.72Ca alloy [17], and is even higher than that of the more concentrated Mg-8Bi-1Al-1Zn sample extruded with similar parameters [13]. Besides, the dilute BX11 alloy by simple one-step extrusion in this study shows much higher strength than that of the Mg-1.32Bi-0.72Ca alloy processed by combining extrusion and caliber rolling [18], which ranks first among all the former reported Mg-Bi-based alloys up to now. Furthermore, compared with the newly developed ultra-high-strength and TX22 alloys [9], the more dilute BX11 alloy shows longer elongation and comparable ultra-high strength.

Table 1. Alloying content (wt.%) and mechanical properties of the BX11 alloy, compared with other typical magnesium alloys [9,11–13].

Alloy	Alloying Content	Tensile Properties			Remark
		TYS (MPa)	UTS (MPa)	EL (%)	
BX11	~2%	394 ± 5.0	411 ± 4.3	6.6 ± 0.6	This study
Mg	~0%	120 ± 3.0	208 ± 2.0	12 ± 2.0	[11]
TX22	~4%	~443	~460	~1.2	[9]
Mg-2Bi	~2%	172 ± 1.0	218 ± 2.0	12.8 ± 0.5	[12]
B6	~6%	189 ± 3.0	228 ± 3.2	19 ± 2.0	[11]
BAZ811	~10%	291 ± 1.0	331 ± 1.0	14.6 ± 0.5	[13]
AZ31	~4%	200 ± 1.0	284 ± 1.0	24.5 ± 0.3	[13]

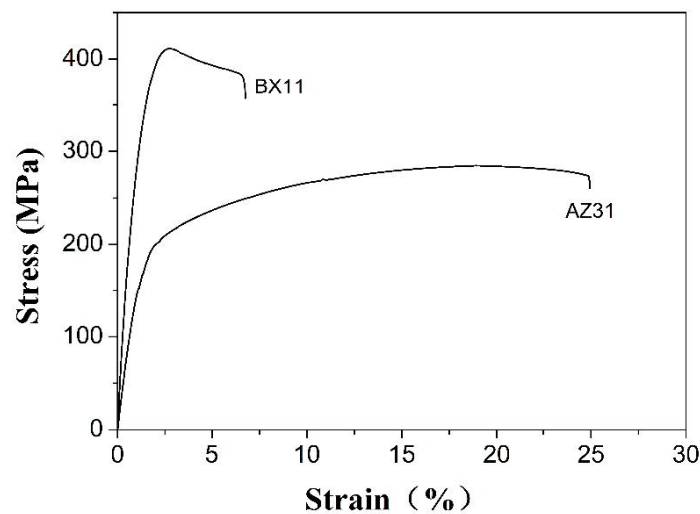


Figure 5. Typical tensile stress–strain curves of the as-extruded BX11 alloy compared with AZ31 [13].

Based on the above microstructure characterization results, the good mechanical properties of the BX11 sample originate from the bimodal microstructure, where fine DRXed grains provide strength, while coarse unDRXed grains enable strain hardening and thus decent ductility [22]. It is well accepted that the submicron grain size can significantly contribute to the high strength according to the Hall–Petch relationship [23]. Compared with AZ31 extruded under similar conditions [13], calculations by the Hall–Petch equation [24] indicate that the contribution to yield strength by grain refinement is 135.0 MPa, demonstrating that the relatively high strength in the BX11 alloy mainly comes from grain refinement. Besides, the strong fiber texture, nano precipitates, micro-sized phases, residual dislocations, sub-grain boundaries, and dissolved solute atoms should also contribute to the resultant high strength. However, it should be noted that the strong fiber texture is detrimental to the formability of the BX11 alloy. Overall, the TYS of the present BX11 alloy with tiny amount of alloying elements additions (~2 wt.%) is among the strongest RE-free Mg alloys. The dilute alloying elements and the simple one-step extrusion are expected to inspire a new alloy design strategy for fabricating high-performance Mg products for larger-scale industrial applications. It is also necessary to further evaluate the anisotropy of the BX11 alloy by preparing the corresponding extruded sheets.

4. Conclusions

In summary, an extraordinary high-strength RE-free BX11 alloy with a TYS of ~394 MPa and elongation of ~6% was successfully fabricated by one-step extrusion. The good mechanical property originates from the bimodal microstructure consisting of ultra-fine DRXed grains and deformed unDRXed grains with residual dislocations and sub-grain boundaries, a strong fiber texture, and homogeneously distributed nano-precipitates. In addition, the formation of sub-micron grains and the evidence for both DDRX and CDRX were also revealed.

Author Contributions: Methodology, S.M., M.Z., and W.Y.; data curation, H.X.; writing—original draft preparation, S.M.; writing—review and editing, S.M., H.X., Z.L., R.J., X.C., L.W., M.Z., and W.Y.; visualization, H.X.; supervision, S.M., W.Y., and L.W.; project administration, S.M.; funding acquisition, S.M. All authors have read and agreed to the published version of the manuscript.

Funding: This work was supported by the Gansu Province Science and Technology Foundation for Youths (Grant No. 21JR7RA261), the Graduate Student Outstanding Innovation Project of Hebei Province (No. CXZZBS2018030), Innovation Fund Project for Universities in Gansu Province (Grant No. 2022A-025), the Project funded by China Postdoctoral Science Foundation (Grant No. 2022M713656), and the Tamarisk Outstanding Young Talents Program of Lanzhou University of Technology.

Institutional Review Board Statement: Not applicable.

Informed Consent Statement: Not applicable.

Data Availability Statement: Not applicable.

Conflicts of Interest: The authors declare no conflict of interest.

References

1. Liu, L.; Wang, J.; Russell, T.; Sankar, J.; Yun, Y. The biological responses to magnesium-based biodegradable medical devices. *Metals* **2017**, *7*, 514. [[CrossRef](#)]
2. Meng, S.; Yu, H.; Fan, S.; Li, Q.; Park, S.H.; Suh, J.S.; Kim, Y.M.; Nan, X.; Bian, M.; Yin, F.; et al. Recent progress and development in extrusion of rare earth free mg alloys: A review. *Acta Metall. Sin.-Engl. Lett.* **2019**, *32*, 145–168. [[CrossRef](#)]
3. Rojas, J.I.; Crespo, D. Onset Frequency of Fatigue Effects in Pure Aluminum and 7075 (AlZnMg) and 2024 (AlCuMg) Alloys. *Metals* **2016**, *6*, 50. [[CrossRef](#)]
4. Zarandi, F.; Yue, S. Magnesium sheet; Challenges and opportunities. In *Magnesium Alloys—Design, Processing and Properties*; Frank, C., Ed.; InTech: London, UK, 2011; ISBN 978-953-307-520-4.
5. Abedini, A.; Butcher, C.; Worswick, M.J. Application of an Evolving non-associative anisotropic-asymmetric plasticity model for a rare-earth magnesium alloy. *Metals* **2018**, *8*, 1013. [[CrossRef](#)]
6. Sravya, T.; Sankaranarayanan, S.; Abdulhakim, A.; Manoj, G. Mechanical properties of magnesium-rare earth alloy systems: A review. *Metals* **2015**, *5*, 1–39.
7. Meng, S.; Dong, L.; Yu, H.; Huang, L.; Han, H.; Cheng, W.; Feng, J.; Wen, J.; Li, Z.; Zhao, W. New ultra-high-strength AB83 alloy by combining extrusion and caliber rolling. *Materials* **2020**, *13*, 709. [[CrossRef](#)] [[PubMed](#)]
8. Meng, S.; Yu, H.; Zhou, J.; Han, H.; Li, Y.; Dong, L.; Nan, X.; Li, Z.; Shin, K.S.; Zhao, W. Enhancing the mechanical properties of AZ80 alloy by combining extrusion and three pass calibre rolling. *Metals* **2020**, *10*, 249. [[CrossRef](#)]
9. Pan, H.; Qin, G.; Huang, Y.; Ren, Y.; Sha, X.; Han, X.; Liu, Z.-Q.; Li, C.; Wu, X.; Chen, H.; et al. Development of low-alloyed and rare-earth-free magnesium alloys having ultra-high strength. *Acta Mater.* **2018**, *149*, 350–363. [[CrossRef](#)]
10. Mohan, R. Green bismuth. *Nat. Chem.* **2010**, *2*, 336. [[CrossRef](#)]
11. Meng, S.J.; Yu, H.; Cui, H.X.; Wang, Z.F.; Zhao, W.M. Microstructure and mechanical properties of extruded pure Mg with Bi addition. *Acta Metall. Sin.* **2016**, *52*, 811–820.
12. Yu, H.; Fan, S.; Meng, S.; Choi, J.O.; Li, Z.; Go, Y.; Kim, Y.M.; Zhao, W.; You, B.S.; Shin, K.S. Microstructural evolution and mechanical properties of binary Mg-xBi (x = 2, 5, and 8 wt%) alloys. *J. Magnes. Alloy.* **2021**, *9*, 983–994. [[CrossRef](#)]
13. Meng, S.; Yu, H.; Zhang, H.; Cui, H.; Park, S.H.; Zhao, W.; You, B.S. Microstructure and mechanical properties of an extruded Mg-8Bi-1Al-1Zn (wt.%) alloy. *Mat. Sci. Eng. A* **2017**, *690*, 80–87. [[CrossRef](#)]
14. Jin, S.-C.; Lee, J.U.; Go, J.; Yu, H.; Park, S.H. Effects of Sn addition on the microstructure and mechanical properties of extruded Mg-Bi binary alloy. *J. Magnes. Alloys* **2022**, *10*, 850–861. [[CrossRef](#)]
15. Liu, Y.; Cheng, W.; Zhang, Y.; Niu, X.; Wang, H.; Wang, L. Microstructure, tensile properties, and corrosion resistance of extruded Mg-1Bi-1Zn alloy: The influence of minor Ca addition. *J. Alloys Compd.* **2020**, *815*, 152414. [[CrossRef](#)]
16. Remennika, S.; Bartschb, I.; Willbold, E.E.; Witte, F.; Shechtman, D. New, fast corroding high ductility Mg-Bi-Ca and Mg-Bi-Si alloys, with no clinically observable gas formation in bone implants. *Mater. Sci. Eng. B* **2011**, *176*, 1653–1659. [[CrossRef](#)]
17. Meng, S.; Yu, H.; Fan, S.; Kim, Y.M.; Park, S.H.; Zhao, W.; You, B.S.; Shin, K.S. A high-ductility extruded Mg-Bi-Ca alloy. *Mater. Lett.* **2020**, *261*, 127066. [[CrossRef](#)]
18. Meng, S.; Yu, H.; Li, L.; Qin, J.; Woo, S.K.; Go, Y.; Kim, Y.M.; Park, S.H.; Zhao, W.; Yin, F.; et al. Effects of Ca addition on the microstructures and mechanical properties of as-extruded Mg-Bi alloys. *J. Alloys Compd.* **2020**, *834*, 155216. [[CrossRef](#)]
19. Meng, S.; Yu, H.; Han, H.; Feng, J.; Huang, L.; Dong, L.; Nan, X.; Li, Z.; Park, S.H.; Zhao, W. Effect of multi-pass caliber rolling on dilute extruded Mg-Bi-Ca alloy. *Metals* **2020**, *10*, 332. [[CrossRef](#)]
20. Wang, Q.H.; Zhai, H.W.; Liu, L.T.; Xia, H.B.; Jiang, B.; Zhao, J.; Chen, D.L.; Pan, F.S. Novel Mg-Bi-Mn wrought alloys: The effects of extrusion temperature and Mn addition on their microstructures and mechanical properties. *J. Magnes. Alloy.* **2021**. [[CrossRef](#)]
21. Yu, H.; Park, S.H.; You, B.S. Development of extraordinary high-strength Mg-8Al-0.5Zn alloy via a low temperature and slow speed extrusion. *Mat. Sci. Eng. A* **2014**, *610*, 445–449. [[CrossRef](#)]
22. Oh-ishi, K.; Mendis, C.L.; Homma, T.; Kamado, S.; Ohkubo, T.; Hono, K. Bimodally grained microstructure development during hot extrusion of Mg-2.4Zn-0.1Ag-0.1Ca-0.16Zr (at.%) alloys. *Acta Mater.* **2009**, *57*, 5593–5604. [[CrossRef](#)]
23. Yu, H.; Xin, Y.; Wang, M.; Liu, Q. Hall-Petch relationship in Mg alloys: A review. *J. Mater. Sci. Technol.* **2018**, *34*, 248–256. [[CrossRef](#)]
24. Jain, A.; Duygulu, O.; Brown, D.W.; Tomé, C.N.; Agnew, S.R. Grain size effects on the tensile properties and deformation mechanisms of a magnesium alloy, AZ31B, sheet. *Mater. Sci. Eng. A* **2008**, *486*, 545–555. [[CrossRef](#)]